Kinematic Synthesis of Stephenson III Six-bar Function Generators

Mark M. Plecnik, J. Michael McCarthy

Robotics and Automation Laboratory
Department of Mechanical and Aerospace Engineering
University of California, Irvine
Irvine, California 92697

Abstract

This paper presents the synthesis of Stephenson III six-bar linkages for function generation. The approach is similar to that of the Stephenson II linkage except additional reductions allow a multihomogeneous degree of 55,050,240 to be computed. A multihomogeneous homotopy was computed for a numerically general system to obtain 834,441 nonsingular solutions which are used to construct efficient parameter homotopies that can be solved for specific function generator task requirements. The linkage solutions found by parameter homotopy are sorted into cognate pairs and analyzed to verify performance. An example is presented of a function generator that creates a specified torque profile to cancel the effects of spasticity in the wrists of stroke survivors.

Keywords:
linkage synthesis, function generator, six-bar

1. Introduction

This paper extends to Stephenson III six-bar linkages the design formulation developed for Stephenson II function generators by Plecnik and McCarthy (2015). In contrast to the Stephenson II, the Stephenson III allows a reduction of the synthesis equations to a polynomial system with multihomogeneous degree 55,050,240. A numerically general system was solved

Email addresses: mplecnik@uci.edu (Mark M. Plecnik), jmmccart@uci.edu (J. Michael McCarthy)

using the polynomial homotopy software BERTINI, Bates et al. (2013); Bertini (2013), running on 512×2.6GHz cores at the San Diego Supercomputer Center of which 834,441 nonsingular solutions were found. These nonsingular solutions were used to construct parameter homotopies for specific synthesis tasks. The parameter homotopies computed in under an hour running on 64×2.2GHz machines of the UC Irvine High Performance Computing Cluster.

The linkage synthesis solutions were sorted into pairs of function generator cognates. It can happen that a cognate solution does not appear in the synthesis results due to numerical issues, in which case those cognates were constructed and added to the synthesis results. Design candidates were analyzed in order to verify performance and find linkages that are free of branch and circuit defects.

An example of the synthesis method is presented by designing a Stephenson III function generator that produces a specified torque profile over the range of its input link, which is used to design a device that cancels the stiffness measured in the wrists of stroke survivors that suffer from spasticity.

2. Literature Review

A six-bar linkage consists of four binary links, that is links with two joints, and two ternary links, links with three joints. These systems form two distinct topologies known as Watt and Stephenson six-bar linkages. The Stephenson six-bar linkages have the property that the two ternary links are separated by the binary links, while the Watt topology has the ternary links connected to each other, Tsai (2000).

The kinematic synthesis of six-bar function generators is a natural extension of the original work by Freudenstein (1954), where the loop equations of the system are formulated in each of the configurations specified by the required input-output angles. Also see Hartenberg and Denavit (1964). This yields a set of polynomial equations in the dimensions of the linkage.

McLarnan (1963) formulated this problem for both Stephenson II and Stephenson III function generators and found solutions for eight positions using the Newton-Raphson method on an IBM 704 computer. In 1994, Dhingra et al. (1994) returned to this problem and solved the synthesis equations for both the Stephenson II and Stephenson III six-bar function generators for nine accuracy positions using a polynomial homotopy algorithm on an IBM 486 PC. This paper solves the 11 accuracy point problem and finds

over 800,000 solutions to the general synthesis equations of which several thousand will pertain to linkage designs in specific cases.

Recent research in the design of six-bar linkages focuses on optimization techniques. Hwang and Chen (2010) used optimization techniques to find defect-free Stephenson II six-bar function generators, while Sancibrian (2011) minimized the difference between the input-output function of the linkage and the desired function. Bulatović et al. (2013) introduced the Cuckoo Search algorithm to design a Stephenson III linkage, and Shiakolas et al. (2005) used a method known as differential evolution.

The synthesis process includes the identification of linkage cognates, Dijksman (1976). The analysis process includes identification of the useful motions each linkage design candidate is capable of producing. The possible motions of a single six-bar linkage can be divided into trajectories that are either bounded on both ends singular configurations or are periodic (corresponding to a fully rotatable input link). Chung (2007) documents the intricacies of six-bar motion.

Planar kinematics are conveniently represented by complex numbers, Erdman et al. (2001). Wampler (1996) showed that it is useful to consider a complex number and its conjugate as *isotropic coordinates* of a point in a plane.

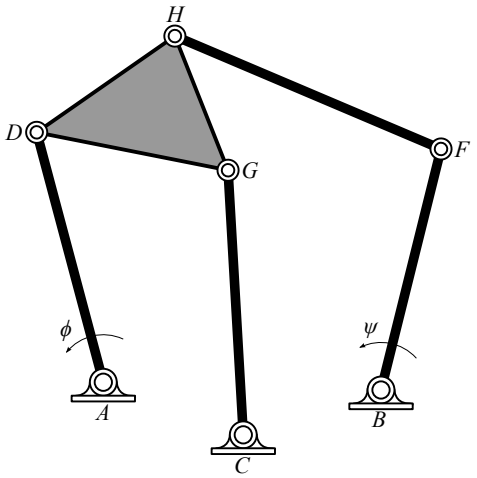

Figure 1: A Stephenson III six-bar function generator.

3. Synthesis Equations for the Stephenson III

The Stephenson III six-bar linkage, Fig. 1, has a ternary link as its ground link, and consists of two loops defined by joint coordinates: (i) $ADGC$, and (ii) $ADHFB$. The ground pivots A and B are used as the centers of N coordinated angles ϕ_j and ψ_j, $j = 0, \ldots, N-1$. The two pivots A and C are part of a four-bar sub-loop, which means their coordinated movement is defined by four-bar loop equations.

To begin we set the scale, orientation, and location of the function generator in the plane by selecting $A = 0 + 0i$ and $D = 1 + 0i$, which defines a reference configuration for the linkage. The coordinates of the remaining joints B, C, F, G and H are calculated by solving the synthesis equations.

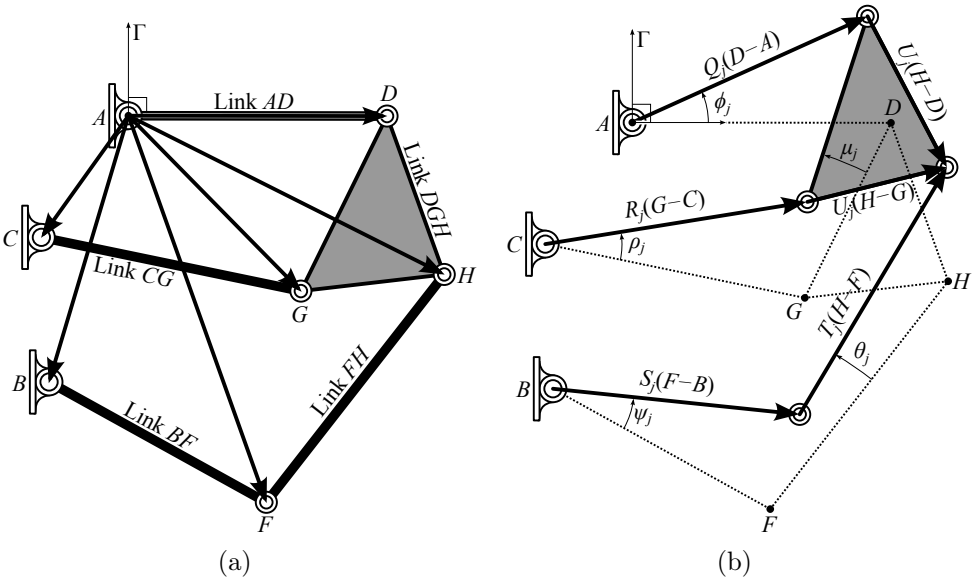

Figure 2: (a) The reference configuration for the synthesis of a Stephenson III function generator. (b) The specified angles of the Stephenson III function generator are measured relative to the reference configuration.

As well, we introduce $(\Delta\phi_j, \Delta\psi_j)$, $j = 1, \ldots, N-1$ as the values of the specified angles measured from the reference configuration, Fig. 2(a), where

$$(\Delta\phi_j, \Delta\psi_j) = (\phi_j - \phi_0, \psi_j - \psi_0), \quad j = 1, \ldots, N-1. \tag{1}$$

The synthesis equations for the Stephenson III linkage are formed from the loop equations obtained for each offset angle pair.

The coordinates of the moving pivots of the Stephenson III six-bar are related to their coordinates in the reference configuration by the equations,

$$\begin{aligned}
D_j =& A + e^{\Delta\phi_j}(D - A),\\
F_j =& B + e^{\Delta\psi_j}(F - B),\\
G_j =& A + e^{\Delta\phi_j}(D - A) + e^{\Delta\mu_j}(G - D),\\
H_j =& A + e^{\Delta\phi_j}(D - A) + e^{\Delta\mu_j}(H - D), \quad j = 1, \ldots, N-1.
\end{aligned} \tag{2}$$

For convenience in what follows, introduce the notation,

$$\begin{aligned}
&Q_j = e^{i\Delta\phi_j}, && R_j = e^{i\Delta\rho_j}, && S_j = e^{i\Delta\psi_j},\\
&T_j = e^{\Delta\theta_j}, && U_j = e^{\Delta\mu_j}, && j = 1, \ldots, N-1.
\end{aligned} \tag{3}$$

Notice that Q_j and S_j are defined by the required angle pairs. The remaining joint angles are unknowns that satisfy the normalization conditions,

$$R_j\bar{R}_j = 1, \quad T_j\bar{T}_j = 1, \quad U_j\bar{U}_j = 1, \quad j = 1, \ldots, N-1. \tag{4}$$

where the overbar denotes the complex conjugate.

The loop equations for the Stephenson III six-bar linkage are obtained by evaluating $G_j - C$ and $H_j - F_j$ relative to the initial configuration. This yields two sets of complex conjugate loop equations,

$$\begin{aligned}
\mathcal{L}_j : R_j(G - C) &= (A + Q_j(D - A) + U_j(G - D)) - C,\\
\bar{R}_j(\bar{G} - \bar{C}) &= (\bar{A} + \bar{Q}_j(\bar{D} - \bar{A}) + \bar{U}_j(\bar{G} - \bar{D})) - \bar{C},\\
&\qquad\qquad j = 1, \ldots, N-1,\\
\mathcal{M}_j : T_j(H - F) &= (A + Q_j(D - A) + U_j(H - D)) - (B + S_j(F - B)),\\
\bar{T}_j(\bar{H} - \bar{F}) &= (\bar{A} + \bar{Q}_j(\bar{D} - \bar{A}) + \bar{U}_j(\bar{H} - \bar{D})) - (\bar{B} + \bar{S}_j(\bar{F} - \bar{B})),\\
&\qquad\qquad j = 1, \ldots, N-1.
\end{aligned} \tag{5}$$

The loop equations $\mathcal{L}_j$, $\mathcal{M}_j$, and the normalization conditions (4) form $7(N-1)$ quadratic equations in the $2(5 + 3(N-1))$ unknowns consisting of the pivots locations B, C, F, G and H and the joint rotations R_j, T_j and U_j and their complex conjugates. The Stephenson III synthesis equations are similar in form to the Stephenson II, and both can be solved for a maximum of $N = 11$ positions to obtain 70 quadratic equations in 70 unknowns that yield a total degree of $2^{70} = 1.18 \times 10^{21}$.

4. Simplification of the Synthesis Equations

The 70 synthesis equations for the Stephenson III function generator can be reduced to 10 equations in 10 unknowns. This can be achieved by eliminating R_j and $\bar{R}_j$ in the pairs of equations $\mathcal{L}_j$ and then eliminating T_j and $\bar{T}_j$ in the pairs of equations $\mathcal{M}_j$ of (5). Finally, the unknowns U_j and $\bar{U}_j$ can be eliminated from the resulting sets of equations, as shown in detail in Plecnik and McCarthy (2015).

To simplify the presentation of this calculation, introduce the complex numbers,

$$\begin{aligned} &a = G - D, \qquad f = G - C, \qquad h = A - C, \qquad k = D - A, \\ &c = H - D, \qquad g = H - F, \qquad m = A - B, \qquad o = -(F - B), \end{aligned} \tag{6}$$

so the loop equations take the form

$$\begin{aligned} \mathcal{L}_j: \quad & h + Q_j k + U_j a - R_j f = 0, \\ & \bar{h} + \bar{Q}_j \bar{k} + \bar{U}_j \bar{a} - \bar{R}_j \bar{f} = 0, \quad j = 1, \ldots, 10, \\ \mathcal{M}_j: \quad & m + Q_j k + U_j c + S_j o - T_j g = 0, \\ & \bar{m} + \bar{Q}_j \bar{k} + \bar{U}_j \bar{c} + \bar{S}_j \bar{o} - \bar{T}_j \bar{g} = 0, \quad j = 1, \ldots, 10. \end{aligned} \tag{7}$$

Eliminate R_j and $\bar{R}_j$ in $\mathcal{L}_j$ and T_j and $\bar{T}_j$ in $\mathcal{M}_j$ to obtain the pairs of equations,

$$\begin{aligned} &(h + Q_j k + U_j a)(\bar{h} + \bar{Q}_j \bar{k} + \bar{U}_j \bar{a}) = f \bar{f}, \\ &(m + Q_j k + U_j c + S_j o)(\bar{m} + \bar{Q}_j \bar{k} + \bar{U}_j \bar{c} + \bar{S}_j \bar{o}) = g \bar{g}, \\ &\qquad\qquad\qquad\qquad j = 1, \ldots, 10. \end{aligned} \tag{8}$$

These 10 pairs of equations are linear in U_j and $\bar{U}_j$, and can be written in the form,

$$\begin{bmatrix} a\bar{b}_j & \bar{a}b_j \\ c\bar{d}_j & \bar{c}d_j \end{bmatrix} \begin{Bmatrix} U_j \\ \bar{U}_j \end{Bmatrix} = \begin{Bmatrix} f\bar{f} - a\bar{a} - b_j\bar{b}_j \\ g\bar{g} - a\bar{a} - d_j\bar{d}_j \end{Bmatrix}, \quad j = 1, \ldots, 10, \tag{9}$$

where the complex numbers $b_j = D_j - C$ and $d_j = D_j - F_j$, given by

$$\begin{aligned} b_j =& h + Q_j k, \\ d_j =& m + Q_j k + S_j o, \qquad j = 1, \ldots, 10. \end{aligned} \tag{10}$$

are introduced to simplify the presentation of these equations.

Eliminate U_j and $\bar{U}_j$ between the pairs of equations (10) in order to obtain,

$$\begin{vmatrix} a\bar{b}_j & f\bar{f} - a\bar{a} - b_j\bar{b}_j \\ c\bar{d}_j & g\bar{g} - a\bar{a} - d_j\bar{d}_j \end{vmatrix} \begin{vmatrix} \bar{a}b_j & f\bar{f} - a\bar{a} - b_j\bar{b}_j \\ \bar{c}d_j & g\bar{g} - a\bar{a} - d_j\bar{d}_j \end{vmatrix} + \begin{vmatrix} a\bar{b}_j & \bar{a}b_j \\ c\bar{d}_j & \bar{c}d_j \end{vmatrix}^2 = 0$$
$$j = 1, \ldots, 10 \qquad (11)$$

where the vertical bars denote the determinant.

The total degree of the polynomial system in Eqn. (11) is $8^{10} = 1.07 \times 10^9$ which is a similar case for the Stephenson II linkage Plecnik and McCarthy (2015). However, the simpler form of Eqn. (10) allows for an additional reduction before employing a multihomogeneous root count.

5. Degree Reduction of the Synthesis Equations

In order to reduce the degree of the synthesis equations (11), introduce the variables,

$$\begin{aligned} r_1 &= a\bar{h}, & r_2 &= c\bar{m}, & r_3 &= c\bar{o}, & r_4 &= m\bar{o}, \\ \bar{r}_1 &= \bar{a}h, & \bar{r}_2 &= \bar{c}m, & \bar{r}_3 &= \bar{c}o, & \bar{r}_4 &= \bar{m}o. \end{aligned} \qquad (12)$$

This allows the expansion of the terms,

$$\begin{aligned} a\bar{b}_j =& r_1 + a\bar{k}\bar{Q}_j, \\ c\bar{d}_j =& r_2 + c\bar{k}\bar{Q}_j + r_3\bar{S}_j, \quad j = 1, \ldots, 10. \end{aligned} \qquad (13)$$

And similarly we expand the rest of the terms in Eqn. (11) using the additional identities $f = a + h + k$ and $g = c + k + m + o$ to find,

$$\begin{aligned} \eta_j =& f\bar{f} - a\bar{a} - b_j\bar{b}_j, \\ =& r_2 + \bar{r}_2 + r_3 + \bar{r}_3 + r_4 + \bar{r}_4 + k(\bar{g} - \bar{k}) + \bar{k}(g - k) \\ & - r_4\bar{S}_j - \bar{r}_4 S_j - kQ_j(\bar{m} + \bar{S}_j\bar{o}) - \bar{k}\bar{Q}_j(m + S_j o), \\ \chi_j =& g\bar{g} - a\bar{a} - d_j\bar{d}_j, \\ =& r_1 + \bar{r}_1 + k(\bar{f} - \bar{k}) + \bar{k}(f - k) - h\bar{k}\bar{Q}_j - \bar{h}kQ_j, \\ & j = 1, \ldots, 10. \end{aligned} \qquad (14)$$

See that k and $\bar{k}$ are known from the specified pivot locations and (Q_j, S_j), $j = 1, \ldots, 10$ are known from the task requirements. Eqns. (13) and (14) are linear in terms of the unknowns a, c, f, g, h, m, o, r_1, r_2, r_3, and r_4.

The synthesis equations (11) can be now be written as,

$$\begin{vmatrix} r_1 + a\bar{k}\bar{Q}_j & \eta_j \\ r_2 + c\bar{k}\bar{Q}_j + r_3\bar{S}_j & \chi_j \end{vmatrix} \begin{vmatrix} \bar{r}_1 + \bar{a}kQ_j & \eta_j \\ \bar{r}_2 + \bar{c}kQ_j + \bar{r}_3 S_j & \chi_j \end{vmatrix} + \begin{vmatrix} r_1 + a\bar{k}\bar{Q}_j & \bar{r}_1 + \bar{a}kQ_j \\ r_2 + c\bar{k}\bar{Q}_j + r_3\bar{S}_j & \bar{r}_2 + \bar{c}kQ_j + \bar{r}_3 S_j \end{vmatrix}^2 = 0, \quad j = 1, \ldots, 10. \tag{15}$$

The result is a set of 10 quartic polynomials, which together with the eight quadratic polynomials, Eqn. (12), yields a polynomial system of degree, $4^{10}2^8 = 268,435,456$.

However, the 18 unknowns in this polynomial system can be separated into the two homogeneous groups,

$$\langle C, \bar{C}, G, \bar{G}, r_1, \bar{r}_1 \rangle, \ \langle B, \bar{B}, F, \bar{F}, H, \bar{H}, r_2, \bar{r}_2, r_3, \bar{r}_3, r_4, \bar{r}_4 \rangle. \tag{16}$$

The number of roots of this system of equations can be calculated as the coefficient of $\alpha_1^6 \alpha_2^{12}$ in the expansion of

$$256\alpha_1^2\alpha_2^6(2\alpha_1 + 2\alpha_2)^{10}, \tag{17}$$

which yields a multihomogeneous degree, 55,050,240. This is a significant reduction in the size of the polynomial homotopy needed to solve these synthesis equations. Multihomogeneous root counting is described in Bates et al. (2013).

6. Solution of the Synthesis Equations

The 18 synthesis equations (12) and (15) were solved on the Gordon cluster at the San Diego Supercomputer Center of the XSEDE supercomputering network using the polynomial homotopy software BERTINI. Rather than specific the requirements for a particular path, the input parameters, (Q_j, S_j), $j = 1, \ldots, 10$, were set to random complex numbers to create a numerically general system. Homotopy paths were tracked over 40 hours on 512×2.6GHz cores. Nonsingular solutions were then sorted out by the Jacobian condition number of which 834,441 were found.

The roots for the general system need only be computed once, and can then be used as the start system for parameter homotopy for any particular

set of input parameters. The advantage of parameter homotopy is that nonsingular endpoints of a general run are used as startpoints of a specific run so that only 834,441 paths need to be tracked in order to find all nonsingular solutions of a specific system.

7. Sorting Solutions

The solutions of the synthesis equations are examined to determine those that have real values for the linkage dimensions. This is checked by ensuring the joint coordinate pairs $(B, \bar{B})$, $(C, \bar{C})$, $(F, \bar{F})$, $(G, \bar{G})$, and $(H, \bar{H})$ are complex conjugates.

Each design candidate is also evaluated to identify its cognate pair among the solutions to the synthesis equations, or to construct the cognate, if it does not appear among these solutions.

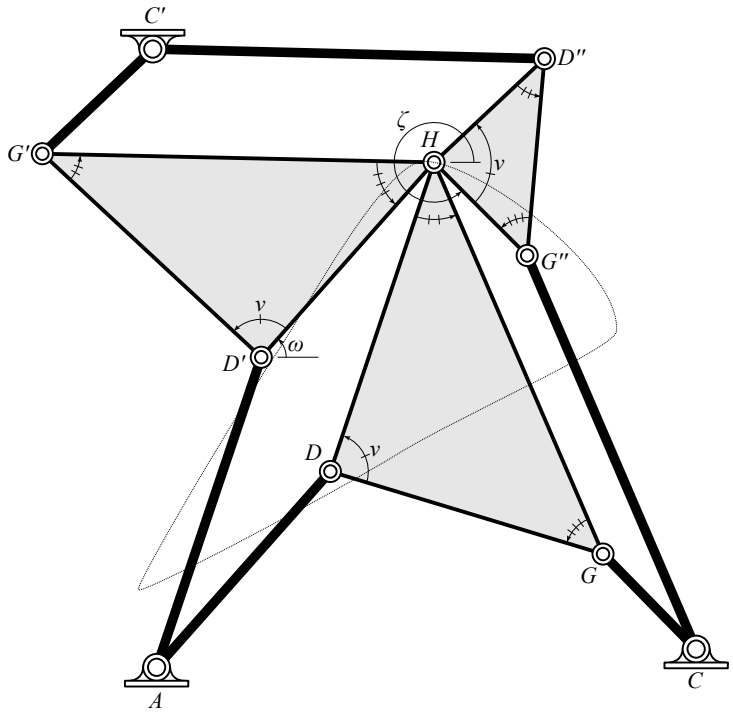

Figure 3: An overconstrained mechanism constructed from three four-bar curve cognates.

7.1. Constructing the Cognates

Dijksman (1976) describes how for every Stephenson III function generator, there exists one other Stephenson III function generator with link lengths of different ratios that produces the exact same function. In order to compute this function generator cognate for a Stephenson III linkage $ABCDFGH$, we consider it as a four-bar linkage $ADGC$ that controls the motion of the RR dyad BF that is connected at H. The four-bar $ADGC$ has two other path cognates that generate the same coupler curve at H (Roberts (1875)), and one of these cognates has an input link that shares the same angular displacement $\Delta\phi$ as Link AD throughout the motion of H (Hartenberg and Denavit (1958)). The Stephenson III function cognate is built from this four-bar path cognate.

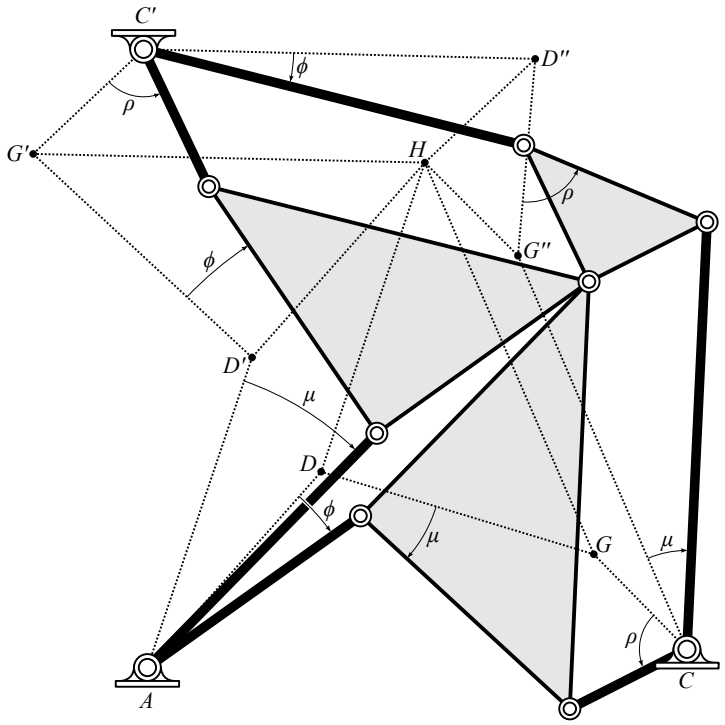

Figure 4: An overconstrained four-bar curve cognate mechanism shown in a displaced configuration.

The four-bar $ADGC$ and its path cognates $AD'G'C'$ and $C'D''G''C$ are shown in Fig. 3 as an overconstrained mechanism that guides the point H. Note that Link $C'D''$ of cognate linkage $C'D''G''C$ shares the same angle $\Delta\phi$

with Link AD as shown in Fig. 4. Therefore, cognate linkage $C'D''G''C$ can be connected to dyad BF at H to form a six-bar function cognate. Following Plecnik and McCarthy (2015), the location of pivots C', D'', and G'' are computed as

$$\begin{aligned} C' &= \frac{(A-D)(G-H)-(C-G)(D-H)}{(G-D)} + H, \\ D'' &= \left(\frac{C-G}{D-G}\right)(D-H) + H, \\ G'' &= C - G + H. \end{aligned} \tag{18}$$

However, our synthesis results only contain linkages with specified pivot locations $A = 0 + 0i$ and $D = 1 + 0i$, so for the sake of comparison, we must scale, rotate, and translate the cognate linkage such that pivots C' and D'' line up with pivots A and D. The transformation which computes this action on a point p is

$$\mathcal{T}(p) = \frac{D-A}{D''-C'}(p-C') + A. \tag{19}$$

or equivalently,

$$\mathcal{T}(p) = \frac{D-G}{H-G}(p-C) + C \tag{20}$$

Applying $\mathcal{T}$ to the cognate linkage, we find the coordinates of six-bar $(ABCDFGH)_c$ as

$$\begin{aligned} A_c &= \mathcal{T}(C') = A \\ B_c &= \mathcal{T}(B) = \frac{D-G}{H-G}(B-C) + C \\ C_c &= \mathcal{T}(C) = C \\ D_c &= \mathcal{T}(D'') = D \\ F_c &= \mathcal{T}(F) = \frac{D-G}{H-G}(F-C) + C \\ G_c &= \mathcal{T}(G'') = D - G + C \\ H_c &= \mathcal{T}(H) = \frac{D-G}{H-G}(H-C) + C \end{aligned} \tag{21}$$

Therefore, for every linkage solution $\{B, C, F, G, H\}$ there should exist another solution $\{B_c, C_c, F_c, G_c, H_c\}$ in the synthesis results. If a missing cognate solution is detected, it is constructed and added to the results.

8. Performance Verification of a Candidate Linkage

Once the design candidates have been sorted into cognate pairs, they are analyzed to evaluate the performance of each design. The criteria for a successful design candidate is the same as was used for the kinematic synthesis of Stephenson II function generators, Plecnik and McCarthy (2015), which is that the required accuracy points lie a single trajectory of configurations without any singularities. Also see Chase and Mirth (1993). This is determined by computing all the configurations of the linkage for a specified range of input angles.

The kinematics equations of the Stephenson III linkage are obtained from the loop equations as,

$$\begin{aligned}
L =& R(G-C) - (A + Q(D-A) + U(G-D)) + C, \\
\bar{L} =& \bar{R}(\bar{G}-\bar{C}) - (\bar{A} + \bar{Q}(\bar{D}-\bar{A}) + \bar{U}(\bar{G}-\bar{D})) + \bar{C}, \\
M =& T(H-F) - (A + Q(D-A) + U(H-D)) + (B + S(F-B)) = 0, \\
\bar{M} =& \bar{T}(\bar{H}-\bar{F}) - (\bar{A} + \bar{Q}(\bar{D}-\bar{A}) + \bar{U}(\bar{H}-\bar{D})) + (\bar{B} + \bar{S}(\bar{F}-\bar{B})) = 0,
\end{aligned} \tag{22}$$

which include the now known initial joint locations,

$$\{A, \bar{A}, B, \bar{B}, C, \bar{C}, D, \bar{D}, F, \bar{F}, G, \bar{G}, H, \bar{H}\} \tag{23}$$

and the unknown joint angle parameters,

$$\{Q, \bar{Q}, R, \bar{R}, S, \bar{S}, T, \bar{T}, U, \bar{U}\}. \tag{24}$$

In the case that the angle ψ of Link BF is the input parameter, then the input $\mathbf{x}$ and output $\mathbf{y}$ variables are

$$\mathbf{x} = (S, \bar{S}), \quad \mathbf{y} = (Q, \bar{Q}, R, \bar{R}, T, \bar{T}, U, \bar{U}), \tag{25}$$

and the analysis equations are

$$\mathbf{F}(\mathbf{x}, \mathbf{y}) = \begin{Bmatrix} L \\ \bar{L} \\ M \\ \bar{M} \\ Q\bar{Q} - 1 \\ R\bar{R} - 1 \\ T\bar{T} - 1 \\ U\bar{U} - 1 \end{Bmatrix} = \begin{Bmatrix} 0 \\ 0 \\ 0 \\ 0 \\ 0 \\ 0 \\ 0 \\ 0 \end{Bmatrix}. \tag{26}$$

These equations have six solutions for a specified input $\mathbf{x} = (S, \bar{S})$ and are easily solved using the *NSolve* function in MATHEMATICA. In the case that the angle ϕ of Link AD is the input parameter, then $\mathbf{x} = (S, \bar{S})$ and Eqns. (25) and (26) change appropriately. The choice of input link provides different parameterizations of the same configuration space and will define different sets of singular configurations. Singular configurations are locations in the configuration space where $\det[J_{\mathbf{F}}(\mathbf{x}, \mathbf{y})] = 0$,

$$[J_{\mathbf{F}}(\mathbf{x}, \mathbf{y})] = \left[\frac{\partial \mathbf{F}}{\partial y_1} \quad \cdots \quad \frac{\partial \mathbf{F}}{\partial y_8} \right]. \tag{27}$$

Singular configurations define the bounds of mechanism branches.

8.1. Sorting the linkage configurations

A set of input parameters $\mathbf{x}_k$, $k = 1, \ldots, n$ is generated that sweeps around the unit circle,

$$\mathbf{x}_k = \left\{ \exp\left((i2\pi) \frac{k-1}{n-1} \right), \exp\left(-(i2\pi) \frac{k-1}{n-1} \right) \right\}, \quad k = 1, \ldots, n. \tag{28}$$

Eqns. (26) are solved for each $\mathbf{x}_k$ to generate n sets of configurations,

$$\mathcal{C}_k = \{(\mathbf{x}_k, \mathbf{y}_{k,1}), \ldots, (\mathbf{x}_k, \mathbf{y}_{k,6})\} \quad k = 1, \ldots, n. \tag{29}$$

The members of $\mathcal{C}_k$ for each k appear in no particular order, and the goal of this section is to sort configurations into separate trajectories as we increment k from 1 to n.

The algorithm initializes by setting the six elements of $\mathcal{C}_1$ as the beginning of six trajectories which are built upon by comparing $\mathcal{C}_k$ to $\mathcal{C}_{k+1}$ and deciphering pairs of connecting configurations,

$$\begin{aligned} \mathcal{C}_k &= \{(\mathbf{x}_k, \mathbf{y}_{k,p}) \mid p = 1, \ldots, 6\}, \\ \mathcal{C}_{k+1} &= \{(\mathbf{x}_{k+1}, \mathbf{y}_{k+1,q}) \mid q = 1, \ldots, 6\}, \end{aligned} \tag{30}$$

where in general configurations $(\mathbf{x}_k, \mathbf{y}_{k,p})$ and $(\mathbf{x}_{k+1}, \mathbf{y}_{k+1,q})$ connect such that $p \neq q$. To decipher connections between $\mathcal{C}_k$ and $\mathcal{C}_{k+1}$, we use Newton's method to solve $\mathbf{F}(\mathbf{x}_{k+1}, \mathbf{y}) = 0$ for $\mathbf{y}$ using start points $\mathbf{y}_{k,p}$, for $p = 1, \ldots, 6$. We name these approximate solutions $\tilde{\mathbf{y}}_{k+1,p}$ where,

$$\tilde{\mathbf{y}}_{k+1,p} = \mathbf{y}_{k,p} - [J_{\mathbf{F}}(\mathbf{x}_{k+1}, \mathbf{y}_{k,p})]^{-1} \mathbf{F}(\mathbf{x}_{k+1}, \mathbf{y}_{k,p}), \quad l = 1, \ldots, 6 \tag{31}$$

is calculated from a single Newton iteration. Multiple iterations are used for more accuracy. The approximate configuration set $\tilde{\mathcal{C}}_{k+1}$ is formed from $\tilde{\mathbf{y}}_{k+1,p}$ where

$$\tilde{\mathcal{C}}_{k+1} = \{(\mathbf{x}_{k+1}, \tilde{\mathbf{y}}_{k+1,p}) \mid p = 1, \ldots, 6\}. \tag{32}$$

Configuration $(\mathbf{x}_k, \mathbf{y}_{k,p})$ of $\mathcal{C}_k$ connects to configuration $(\mathbf{x}_{k+1}, \mathbf{y}_{k+1,q})$ of $\mathcal{C}_{k+1}$ if the following condition evaluates as true,

$$|\tilde{\mathbf{y}}_{k+1,p} - \mathbf{y}_{k+1,q}| < \text{tol}, \tag{33}$$

where tol is a specified threshold value. For most k, configurations $\mathcal{C}_k$ and $\mathcal{C}_{k+1}$ will connect in a one to one fashion. However, Eqn. (33) allows the possibility that a configuration of $\mathcal{C}_k$ will connect to several or none of the configurations of $\mathcal{C}_{k+1}$, which is often the case near singularities. In these cases, we employ the following logic:

1. If a configuration of $\mathcal{C}_{k+1}$ is not connected to a configuration of $\mathcal{C}_k$, that configuration of $\mathcal{C}_{k+1}$ begins a new trajectory.
2. If a configuration of $\mathcal{C}_k$ connects to multiple configurations of $\mathcal{C}_{k+1}$, the trajectory associated with the configuration of $\mathcal{C}_k$ is duplicated and each duplicate connects to a matching element of $\mathcal{C}_{k+1}$.
3. If a configuration of $\mathcal{C}_k$ does not connect to any configurations of $\mathcal{C}_{k+1}$, the trajectory associated with the configuration of $\mathcal{C}_k$ is concluded.

This procedure is executed for a complete sweep of the unit circle $\mathbf{x}_k$, $k = 1, \ldots, n$, such that $\mathbf{x}_n = \mathbf{x}_1$. The result of this algorithm is a set of connected sequences of configurations that form separate mechanism trajectories. All combinations of these trajectories are checked for connections from $k = n$ to $k = 1$ configurations. If connections are identified, these trajectories are chained together to form longer trajectories.

Finally, configurations that do not correspond to rigid body movement are removed, and the determinant of the Jacobian matrix along each configuration is evaluated. A sign change indicates a change in configuration that can arise from numerical error.

8.2. Identifying successful designs

Once all trajectories have been assembled for a linkage design candidate, each is checked to see which and how many of the specified accuracy points they contain. A successful design candidate will produce a trajectory that

moves through all 11 accuracy points. We term these designs 11-point mechanisms.

While linkage designs that contain all 11 accuracy points on a single trajectory is the goal, our design process identifies linkage designs with trajectories that move through less than 11 points as well. It is often the case that these mechanisms only slightly miss some accuracy points and may have other features useful to the designer, such as compact dimensions or reduced link overlap.

9. Design of a Torque Cancelling Linkage

Survivors of strokes often suffer from a muscle control disorder called spasticity which causes increased stiffness in muscles of joints such as the wrist. Measurement data of intrinsic wrist stiffness can be found in Mirbagheri and Settle (2010), and shown in Fig. 5. The goal is to design a six-bar linkage that generates a specified torque profile which cancels spastic wrist stiffness.

9.1. Obtaining the input torque profile

The torque profile that the Stephenson III is to reproduce, and then cancel, is derived from the data collected by Mirbagheri and Settle (2010), who measured the intrinsic stiffness profile in the wrists of 21 stroke survivors. The data was taken from the graph they provided and was least-squares fit with the following fifth degree polynomial,

$$\begin{aligned} S(x) = &-0.3403347740344527x^5 + 2.3767146714792213x^4 \\ &+ 1.4329074166324411x^3 - 0.21211179259258692x^2 \\ &+ 0.5381754676253262x + 1.903537638831755. \end{aligned} \tag{34}$$

Because stiffness is the rate of change of a spring torque with respect to angular deflection, we integrate $S(x)$ to obtain the torque profile,

$$\begin{aligned} T(x) = \int S(x)dx + c_0 = &-0.056722462339075x^6 + 0.475342934295844x^5 \\ &+ 0.358226854158110x^4 - 0.070703930864196x^3 + 0.269087733812663x^2 \\ &+ 1.903537638831755x + 1.859723104149862. \end{aligned} \tag{35}$$

Eqns. (34) and (35) are shown in Fig. 5. The integration constant of the torque profile was set such that $T(-\pi/3) = 0$ which requires an unstable

equilibrium at $x = -\pi/3$ rad. That means when the input link is rotated in the positive direction, a positive torque will act on it and move the link away from the equilibrium position. Thus, this linkage will behave like a spring with negative stiffness.

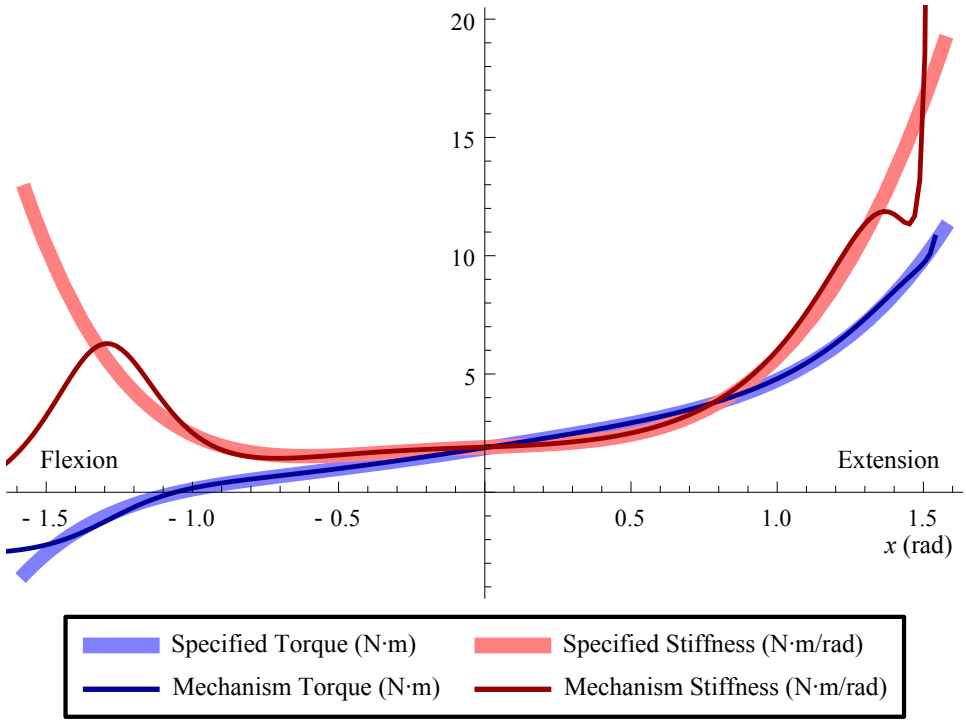

Figure 5: Desired torque and stiffness profiles as derived from Mirbagheri and Settle (2010) and the torque and stiffness profiles produced by the example mechanism. As well, the resultant torque taken by negating the mechanism generated torque from the desired torque.

9.2. Input-output function

The use of a function generator to provide a required input torque profile begins with the assumption that there are no losses from friction, wear, and dynamic effects, this yields the power balance,

$$T_{in}\dot{x} = T_{out}\dot{y}, \tag{36}$$

where $\dot{x}$ denotes the angular velocity of the input crank, and $\dot{y}$ is the angular velocity of the output crank.

Table 1: Task position data as displayed in Fig. 6.

j	x_j	y_j
1	$-90°$	$-6.665566873543°$
2	$-68°$	$-19.185437363846°$
3	$-45°$	$-18.280827185669°$
4	$-22°$	$-11.558672810110°$
0	$0°$	$0°$
5	$19°$	$15.000375068384°$
6	$37°$	$34.756261256578°$
7	$54°$	$61.184689516866°$
8	$70°$	$99.804701760596°$
9	$82°$	$148.305746675651°$
10	$90°$	$203.021804302295°$

For this design, the output torque T_{out} is generated by a torsion spring with stiffness k and equilibrium angle y_e, therefore the input torque is given by,

$$T_{in} = -k(y - y_e)\frac{\dot{y}}{\dot{x}} = -k(y - y_e)\frac{dy}{dx}, \tag{37}$$

which is a function of the input angle x. Eqn. (37) can be solved for $y = f(x)$ to obtain the set of input-output angles needed to design a Stephenson III function generator.

Separate variables and integrate to obtain,

$$-\frac{1}{k}\int T_{in}(x)dx = \frac{1}{2}y^2 - y_e y \tag{38}$$

and then solve for y to obtain,

$$y = f(x) = \pm\sqrt{-\frac{2}{k}\int T_{in}(x)dx + y_e^2} + y_e. \tag{39}$$

The "+" and "−" solutions are two different functions that produce the desired torque profile for given spring parameters k and y_e.

The input-output function for the synthesis of the Stephenson III function generator is obtained by substituting (35) into (39), with the requirement that $k = 0.45$ N·m/rad and $y_e = 2\pi$ rad. The "−" solution was taken to calculate the input-output $y = f(x)$ function shown in Figs. 6(b) and 6(d).

Table 2: Synthesis results for the cases of actuating Link AD, $\psi = f(\phi)$, and actuating Link BF, $\phi = f(\psi)$.

	$\psi = f(\phi)$	$\phi = f(\psi)$
Linkage solutions	8341	8583
Cognates added	712	647
Linkages analyzed	4547	5323
11 point mechanisms	96	109
10 point mechanisms	225	131
9 point mechanisms	352	333
8 point mechanisms	450	596
7 point mechanisms	793	887
6 point mechanisms	1389	1104
Synthesis computation time (hr)	0.8	0.9
Analysis computation time (hr)	4.0	6.1

This input-output function was evaluated at 11 positions of x to obtain the coordinated angles shown in Table. 1. We investigate producing this function using both AD as the input, $(x, y) = (\Delta\phi, \Delta\psi)$, and BF as the input, $(x, y) = (\Delta\psi, \Delta\phi)$. The use of BERTINI to obtain solutions to the synthesis equations is the same for both cases.

9.3. Successful linkage designs

A summary of synthesis results is shown in Table 2. For the cases with ϕ as the input and ψ as the input, BERTINI found 8,341 and 8,583 solutions that corresponded to physical linkages, respectively. Each solution set was then processed to add cognate solutions and remove solutions with very small or large link lengths such that 4,547 and 5,323 solutions were prepared for each case. The performance of these linkages was analyzed in order to categorize mechanisms by the number of accuracy points they can achieve in a singularity-free trajectory from 6 to 11 points. For ϕ as the input and ψ as the input, there were 96 and 109 mechanisms, respectively, that passed through all 11 points. The total computation time for each case was 5 hrs and 7 hrs performed on 64×2.2GHz nodes of the UC Irvine High Performance Computing Cluster.

Fig. 6 shows two 11–point mechanisms and their input-output functions, one with ϕ as the input and one with ψ as the input. Fig. 5 shows the torque and stiffness profiles produced by the linkage shown in Fig. 6(a).

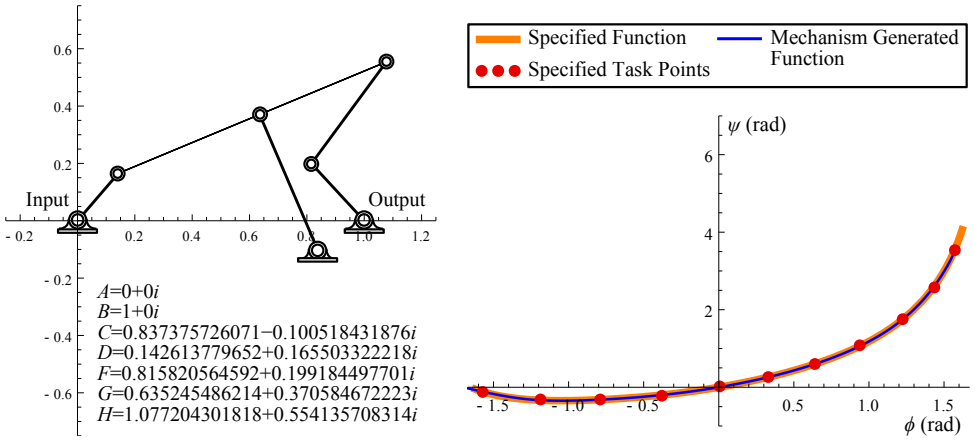

(a) $\Delta\phi$ is input (b) $\Delta\psi = f(\Delta\phi)$

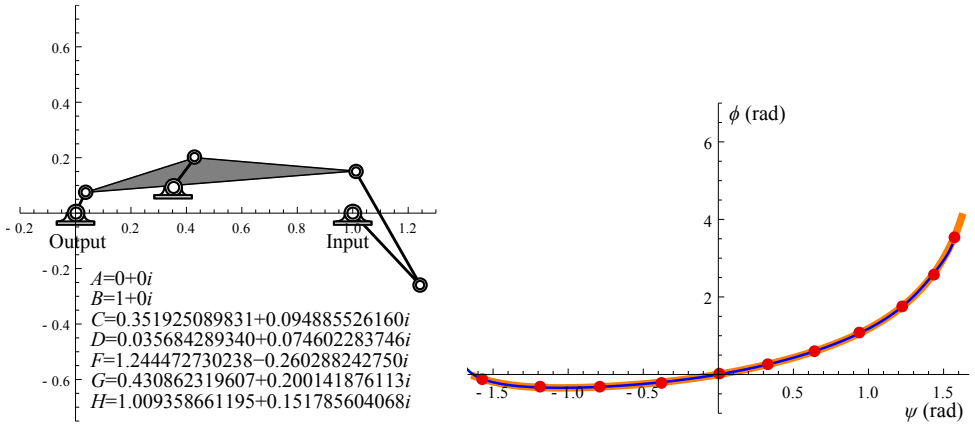

(c) $\Delta\psi$ is input (d) $\Delta\phi = f(\Delta\psi)$

Figure 6: (a) A Stephenson III linkage actuated by Link AD and (b) its mechanized function and (c) a Stephenson III linkage actuated by Link BF and (d) its mechanized function.

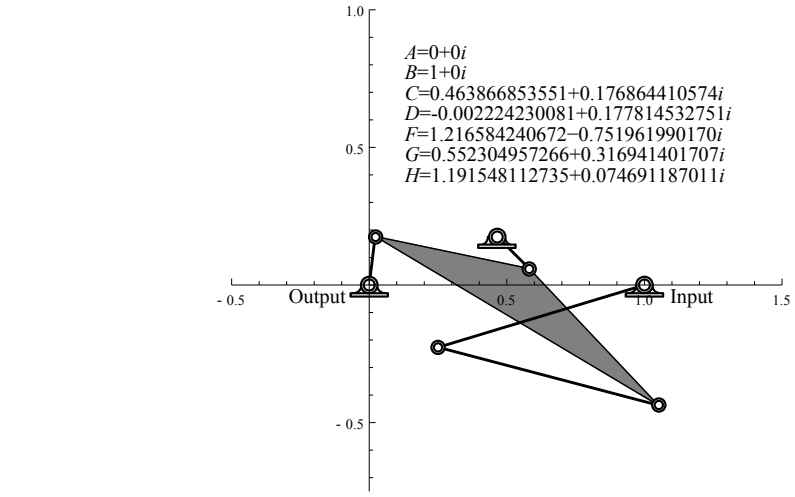

(a)

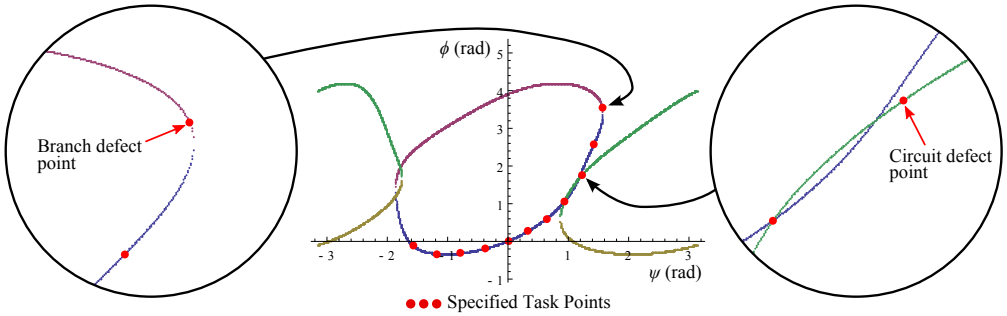

(b)

Figure 7: (a) A defective linkage and (b) its configuration space. Separate singularity free trajectories are indicated with different colors. A branch and circuit defect is illustrated.

Fig. 7 illustrates some common defects found in mechanisms that achieve less than 11 accuracy points. The figure depicts the configuration of a 9–point mechanism. Notice that one accuracy point is on a separate trajectory yielding a circuit defect. However, in the second case the accuracy point is on the same trajectory but separated from the others by a singularity, known as a branch defect. Despite these defects, the mechanism tracks the desired trajectory very closely and is useful to the designer.

9.4. Example design

A solid model of the 11–point mechanism shown in Fig. 6(a) was produced and is shown in Figs. 8 and 9. This device can be used to cancel the torque

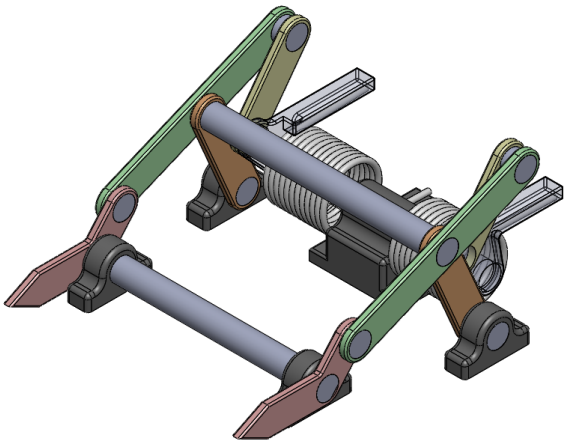

Figure 8: An embodiment of the design shown in Fig. 6(a).

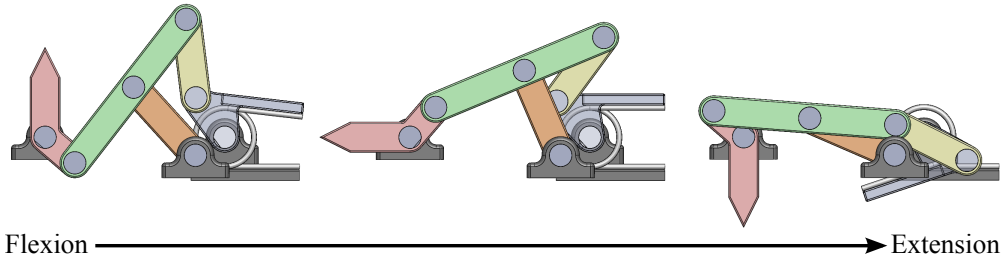

Figure 9: An embodiment of the design shown in Fig. 6(a) shown in three poses.

that arises from the intrinsic stiffness of stroke survivors that suffer from spasticity. The negation of the mechanism generated torque from the stroke survivor data yields a resultant torque near zero shown in Fig. 10.

10. Conclusions

This paper presents a synthesis procedure for Stephenson III six-bar function generators that achieve 11 coordinated input and output angles. It is shown that the structure of the synthesis equations yields a polynomial system with multihomogeneous degree of 55,050,240. The polynomial homotopy software BERTINI was used to compute 834,441 nonsingular solutions for a general set of parameters. These solutions were then used in a parameter homotopy to obtain the dimensions of Stephenson III six-bar function generators. Each solution is analyzed to ensure its performance, and it is shown

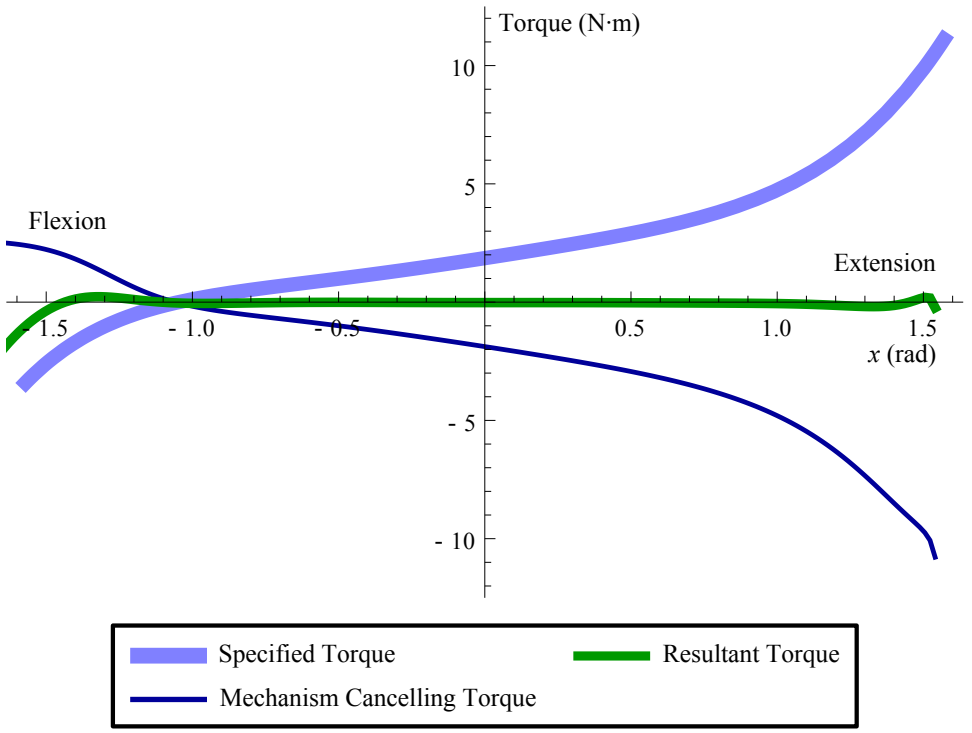

Figure 10: The resultant of the desired torque and the torque generated by the mechanism shown in Fig. 6(a) is near zero.

that successful designs may have small errors at specific accuracy points. An example design uses the Stephenson III linkage to transform a linear spring on the output into a torque profile on the input that cancels the intrinsic stiffness of the wrist of a stroke survivor.

11. Acknowledgments

This material is based upon work supported by the National Science Foundation under Grant No. CMMI 1066082.

12. References

S. S. Balli and S. Chand, 2002. "Defects in link mechanisms and solution rectification," *Mechanism and Machine Theory* 37(9): 851-876.

D. J. Bates, J. D. Hauenstein, A. J. Sommese, and C. W. Wampler. Bertini: Software for Numerical Algebraic Geometry. Available at bertini.nd.edu with permanent doi: dx.doi.org/10.7274/R0H41PB5.

D. J. Bates, J. D. Hauenstein, A. J. Sommese, and C. W. Wampler, 2013. *Numerically Solving Polynomial Systems with Bertini*, SIAM Press, Philadelphia, PA.

R. R. Bulatović, S. R. Đorđević and V. S. Đorđević, 2013. "Cuckoo Search algorithm: A metaheuristic approach to solving the problem of optimum synthesis of a six-bar double dwell linkage," *Mechanism and Machine Theory*, 61:1–13.

T. R. Chase and J. A. Mirth, 1993. "Circuits and branches of single-degree-of-freedom planar linkages," *Journal of Mechanical Design*, 115(2):223-230.

W. Y. Chung, 2007. "Double configurations of five-link Assur kinematic chain and stationary configurations of Stephenson six-bar," *Mechanism and Machine Theory*, 42(12): 1653–1662.

A. K. Dhingra, J. C. Cheng, and D. Kohli, 1994. "Synthesis of six-link, slider-crank and four-link mechanisms for function, path and motion generation using homotopy with m-homogenization", *Journal of Mechanical Design*, 116(4):1122-1131.

E. A. Dijksman, 1976. *Motion Geometry of Mechanisms*, Cambridge University Press, London.

A. G. Erdman, G. N. Sandor, and S. Kota, 2001. *Mechanism Design: Analysis and Synthesis*, Prentice Hall, Upper Saddle River, NJ.

F. Freudenstein, 1954. "An analytical approach to the design of four-link mechanisms", *Transactions of the ASME*, 76:483-492.

R. S. Hartenberg, and J. Denavit, 1964. *Kinematic Synthesis of Linkages*, McGraw-Hill, New York, NY.

R. S. Hartenberg and J. Denavit, 1958. "The fecund four-bar linkage," *Transactions of the Fifth Mechanism Conference*, Purdue University, Lafayette, Indiana, pp. 194–206.

W. M. Hwang and Y. J. Chen, 2010. "Defect-Free Synthesis of Stephenson-II Function Generators", *Journal of Mechanisms and Robotics*, 2(4):041012.

C. W. McLarnan, 1963. "Synthesis of six-link plane mechanisms by numerical analysis", *Journal of Engineering for Industry*, 85(1):5-10.

M. M. Mirbagheri and K. Settle, 2010. "Neuromuscular properties of different spastic human joints vary systematically", *32nd Annual International Conference of the IEEE EMBS*, Buenos Aires, Argentina.

M. Plecnik and J. M. McCarthy, "Computational Design of Stephenson II Six-bar Function Generators for 11 Accuracy Points," under review for the ASME Journal of Mechanisms and Robotics, March 2015.

M. Plecnik and J. M. McCarthy, 2014. "Numerical Synthesis of Six-bar Linkages for Mechanical Computation," *ASME Journal of Mechanisms and Robotics*, 6(3): 031012.

S. Roberts, 1875. "Three-bar Motion in Plane Space", Proceedings of the London Mathematical Society s1-7(1):14-23.

R. Sancibrian, 2011. "Improved GRG method for the optimal synthesis of linkages in function generation problems", *Mechanism and Machine Theory*, 46(10):1350-1375.

P. S. Shiakolas, D. Koladiya, and J. Kebrle, 2005. "On the optimum synthesis of six-bar linkages using differential evolution and the geometric centroid of precision positions technique," *Mechanism and Machine Theory*, 40(3):319–335.

P. A. Simionescu, and M. R. Smith, 2001. "Four-and six-bar function cognates and overconstrained mechanisms", *Mechanism and machine theory* 36(8):913-924.

L. W. Tsai, 2000. *Mechanism Design: Enumeration of Kinematic Structures According to Function*, CRC Press.

C. W. Wampler, 1996. "Isotropic coordinates, circularity, and Bézout numbers: planar kinematics from a new perspective," *Proceedings of the 1996 Design Engineering Technical Conferences*, 96-DETC/MECH-1210, Irvine, CA.